

An expert-system to control the CFL number of implicit upwind methods

Denis Vanderstraeten, Árpád Csík and Dirk Roose

Report TW 304, March 2000



Katholieke Universiteit Leuven
Department of Computer Science
Celestijnenlaan 200A – B-3001 Heverlee (Belgium)

An expert-system to control the CFL number of implicit upwind methods

Denis Vanderstraeten, Árpád Csík and Dirk Roose

Report TW 304, March 2000

Department of Computer Science, K.U.Leuven

Abstract

Direct implicit simulation of complex steady state flows is usually too difficult numerically in the absence of a good initial guess. “Pseudo-transient-continuation” is a physically motivated technique that follows the physical transient solution starting from a uniform flow. Here, a delicate choice of the time steps, or the CFL numbers is crucial to reduce the number of iterations. However, existing strategies such as exponential laws (EXP) or residual-norm based strategies (SER) are not robust; if some initial parameters are not carefully chosen, they may produce an excessive number of iterations or produce non-physical states (breakdowns).

In this paper, we investigate this problem and propose an *expert-system* for the automatic determination of the CFL numbers. This expert-system uses several metrics to estimate the convergence rate and the possibility of breakdowns. It then takes the appropriate actions. Numerical results obtained on a wide variety of test cases show a systematic reduction of the total number of iterations compared to SER or EXP. Furthermore, the system seems more robust in the sense that iteration counts depend only slightly on the parameters, and breakdowns are avoided while convergence is almost guaranteed.

Keywords : CFL number, implicit method, convergence rate, hyperbolic systems.

An expert-system to control the CFL number of implicit upwind methods

DENIS VANDERSTRAETEN¹ AND ÁRPÁD CSÍK² AND DIRK ROOSE¹

Abstract

Direct implicit simulation of complex steady state flows is usually too difficult numerically in the absence of a good initial guess. “Pseudo-transient-continuation” is a physically motivated technique that follows the physical transient solution starting from a uniform flow. Here, a delicate choice of the time steps, or the CFL numbers is crucial to reduce the number of iterations. However, existing strategies such as exponential laws (EXP) or residual-norm based strategies (SER) are not robust; if some initial parameters are not carefully chosen, they may produce an excessive number of iterations or produce non-physical states (breakdowns).

In this paper, we investigate this problem and propose an *expert-system* for the automatic determination of the CFL numbers. This expert-system uses several metrics to estimate the convergence rate and the possibility of breakdowns. It then takes the appropriate actions. Numerical results obtained on a wide variety of test cases show a systematic reduction of the total number of iterations compared to SER or EXP. Furthermore, the system seems more robust in the sense that iteration counts depend only slightly on the parameters, and breakdowns are avoided while convergence is almost guaranteed.

Keywords: CFL number, implicit method, convergence rate, hyperbolic systems.

1 Introduction

In nature, laboratory and industry many processes can be described by hyperbolic conservation laws, with or without a source term. The set of Euler, Navier-Stokes or Magnetohydrodynamic equations can be viewed as special instances of hyperbolic PDE’s. Their generic form is written as

$$\frac{\partial U}{\partial t} + \nabla \cdot \mathbf{F} = S, \quad (1)$$

where the vector U contains the unknown quantities of the problem (*e.g.* density, momentum vector and total energy density in the case of the Euler equations), \mathbf{F} stands for the convective flux vector and the source term S usually describes non-ideal (dissipative) effects, external forces, heating terms, sources or sinks of certain physical quantities.

¹Katholieke Universiteit Leuven, Department Computer Science, Celestijnenlaan, 200A, B-3001 Heverlee (Belgium), e-mail: denis@cs.kuleuven.ac.be

²von Karman Institute, Chaussée de Waterloo, 72, B-1640 Rhode-St-Genèse (Belgium) and e-mail: arpi@vki.ac.be / Katholieke Universiteit Leuven, Department of Mathematics, Celestijnenlaan, 200B, B-3001 Heverlee (Belgium)

Equation (1) constitutes a set of highly nonlinear partial differential equations. In the vast majority of industrial and scientific applications the full set of governing equations has to be solved, usually on complex geometries. There exists a wide variety of numerical techniques to approximate the solution of the PDE's, such as finite difference, finite volume, finite element, spectral and residual distribution methods, just to name a few of them. In each of these methods the spatial operator is discretized by using different numerical principles. However, after applying the spatial discretization operator on the equations, all of them can be cast in the simple form

$$\frac{dU}{dt} = -R(U), \quad (2)$$

where the vector $U = U(t)$ now represents the spatial discretization of the solution vector and $R(U)$ is called the *residual* vector. If the transient phenomena are not of interests, (2) can be substituted by the set of non-linear algebraic equations

$$R(U) = 0. \quad (3)$$

However, in the absence of a sufficiently good initial approximation, Newton's method applied to (3) will generally not converge. Other methods like fixed point methods or globalization techniques such as trust region methods or line search algorithms are also likely to fail or to stagnate in a local minimum of $\|R(U)\|$ [1, 2]. The usual alternative is to keep (2) as a time dependent problem and to march to the steady state by following the physical transient in time (see [3] and the references therein).

Explicit time integration techniques, achieved by a linear combination of the iterate at previous time steps are robust, straightforward and require few parameters. However, they appear prohibitively time consuming on complex problems due to stability constraints. Implicit iterative methods are known to remain stable even for large values of the time step. "Yet, there is no clear understanding as what the optimal time-increment should be at each time level for a given flow configuration. This fact is all the more embarrassing that the choice of an inadequate time-increment can be extremely detrimental to the overall convergence performance" [4]. The aim of this paper is to understand the time step requirements for the implicit technique and provide a *time-stepping strategy* with enhanced convergence properties. To this end, the backward Euler integration is applied to the set of non-linear algebraic equations

$$\frac{\Delta U^{(k)}}{\Delta t^{(k)}} = -R(U^{(k+1)}).$$

The superscript k denotes the (non-linear) iteration number while $\Delta t^{(k)}$ is the time step and $\Delta U^{(k)} = U^{(k+1)} - U^{(k)}$ is the correction to the approximate solution. The right-hand-side is then linearized by a Taylor expansion truncated to the first order. Hence, every non-linear iteration k requires the solution of a linear system of the form

$$\left(\frac{1}{\Delta t^{(k)}} I + J^{(k)} \right) \Delta U^{(k)} = -R(U^{(k)}),$$

where the matrix $J^{(k)}$ is the Jacobian matrix of R evaluated at $U^{(k)}$ and I is the identity.

If the transient states are not of interest, a local time stepping technique may be used. The numerical stability of the scheme requires a maximum time step controlled by a so-called CFL number. The previous expression is generalized in

$$\left(\frac{1}{\gamma^{(k)}} D^{(k)} + J^{(k)} \right) \Delta U^{(k)} = -R(U^{(k)}), \quad (4)$$

where the diagonal matrix $D^{(k)}$ contains the local time steps and $\gamma^{(k)}$ is the CFL number. In the following, the linear system (4) is also written as

$$M^{(k)} \Delta U^{(k)} = -R^{(k)}.$$

In this paper, we focus on the problem of finding a *robust* strategy for the determination of $\gamma^{(k)}$ ensuring a *quasi-minimum* number of iterations to reach the steady-state solution. This problem is heuristic in nature and therefore, we propose an *expert-system* that attempts to understand the features of the problem. This system keeps track of important metrics of the iteration history (such as the norm of the residual vector) to decide whether to increase or decrease $\gamma^{(k)}$ and by which amount. Robustness is obtained by detecting possible breakdowns³ at early stages and taking smaller subsequent CFL numbers. Furthermore this new expert-system does not depend on some initial parameters which denotes, again, an increased robustness.

Compared to existing strategies such as the SER or the exponential strategies [5, 6], a faster convergence has consistently been observed on a wide variety of test cases. Furthermore, the expert-system is more robust in the sense that no breakdowns occur and the total number of non-linear iterations depends only slightly on the parameters.

The remainder of this paper is organized as follows. Section 2 describes two existing strategies, namely SER and EXP and emphasizes both advantages and weaknesses. Section 3 details the heuristics of the expert-system and presents its physical motivation. The particular upwind discretization method, used in the numerical experiments, is briefly sketched in Section 4. The experiments on several representative test cases are described and commented in Section 5.

2 Review of usual strategies

Literature on optimal strategies for the CFL number is somewhat limited [5, 6, 7, 8]. Some strategies do not take into account the convergence history or the problem itself while other techniques attempt to incorporate some knowledge of the problem although in a limited way. Also, to our knowledge, no strategy has been proposed to address the issue of breakdowns. Most authors simply restart the

³A breakdown occurs when the solution becomes non-physical, for example with negative density, ...

iterations from scratch with adapted values of the parameters when a breakdown occurs.

Existing strategies are usually based on the following rules of thumb: the time step should remain small until all flow features are sufficiently resolved and large time steps may be taken near the solution to obtain super-linear or quadratic convergence of Newton’s method. Also, some authors suggest to set a bound on the maximum CFL number for conditioning reasons. We discuss two strategies and show advantages and weaknesses.

2.1 Switch Evolution Relaxation

The Switch Evolution Relaxation (SER) strategy

$$\gamma^{(k)} = \gamma_{SER} \frac{\|R(U^{(0)})\|_2}{\|R(U^{(k)})\|_2}$$

is a common technique to increase the CFL number as convergence proceeds [5, 6]. Unfortunately, the user-defined initial parameter γ_{SER} is crucial for the success of the strategy. Indeed, if the residual norm stays close to $\|R(U^{(0)})\|_2$ at the beginning of the iteration, $\gamma^{(k)}$ remains also close to γ_{SER} . For small value of this parameter, the matrix $M^{(k)}$ has large diagonal coefficients and the iterative scheme (4) resembles to an explicit scheme with slow convergence. This convergence affects $\|R(U^{(k+1)})\|_2$, and, in turn, $\gamma^{(k+1)}$. There is thus a vicious circle that slows down the entire convergence and results in many unnecessary iterations.

Another drawback encountered with the SER strategy is the presence of oscillations. A rapid decrease of the residual norm produces a jump of $\gamma^{(k+1)}$. For a large $\gamma^{(k+1)}$, the matrix $M^{(k+1)}$ is close to $J^{(k+1)}$. If the iterate is far from the solution, the new direction

$$\Delta U^{(k)} = M^{(k)-1} R^{(k)} \simeq J^{(k)-1} R^{(k)}$$

may not be a descent direction, resulting in a large residual norm at iteration $k+2$. This phenomenon creates an oscillation that may propagate for several iterations.

2.2 Exponential law

The exponential law (EXP)

$$\gamma^{(k)} = (\gamma_{EXP})^k$$

increases the CFL number in a regular manner [9]. Unlike the SER strategy, the exponential constantly “pushes” the CFL to large values in an attempt to speed up convergence. Also, the smoothness of the exponential reduces the apparition of oscillations. The price to pay is the absence of control of the strategy by the problem itself. It is the user’s responsibility to effectively tune the parameter.

Similar to SER, the value of the initial parameter is also important. For some problems, a very small γ_{EXP} may be required to avoid breakdowns during the first iterations. Then, near the solution, $\gamma^{(k)}$ remains small even if larger values could be selected to increase the convergence speed.

3 An Expert System to adapt the CFL

Existing strategies ensure global convergence by selecting small CFL numbers for the early iterations, allowing $\gamma^{(k)}$ to grow as the iterate approaches the solution. They may produce oscillations, slow convergence or even breakdowns. Oscillations appear if the CFL number is directly proportional to some problem-dependent metric while slow convergence is the result of an underestimated initial parameter. Breakdowns happen when the physical transient is not accurately followed due to instabilities caused by large CFL numbers.

These considerations define the key ingredients for an effective and robust strategy:

- The convergence history can be split in two distinct phases with different properties: an *initial* and a *terminal* phases. In [3], three phases are proposed.
- Breakdowns or possible breakdowns need to be detected early to allow a reduction of the CFL number in the initial phase.
- The convergence rate must be estimated ensuring large $\gamma^{(k)}$ in the terminal phase.

We have chosen a piecewise exponential function to satisfy these goals. In its simplest form, the CFL numbers are determined by only two exponential functions. The first function corresponds to the initial phase. In this phase, the CFL numbers must remain small and the parameter γ_0 is close to 0. During the terminal phase, all flow features are resolved and a fast convergence rate may be expected. A faster growing exponential function may be taken ($\gamma_1 > \gamma_0$). The CFL numbers are recursively defined by

$$\gamma^{(k)} = \begin{cases} (1 + \gamma_0) \gamma^{(k-1)} & \text{if } k < k_{switch}, \\ (1 + \gamma_1) \gamma^{(k-1)} & \text{if } k \geq k_{switch}. \end{cases} \quad (5)$$

where the iteration k_{switch} separates the initial and terminal phases. The two multipliers γ_0 and γ_1 as well as the iteration index k_{switch} need to be estimated by the expert-system. Finally, as advocated by other authors in the case of the SER or exponential strategies, the maximum CFL number is limited by a given value γ_{max} .

3.1 Initial phase

In general, one single exponential in the initial phase is not sufficient to avoid breakdowns while ensuring reasonable convergence rate. Indeed, a large value of γ_0 may result in a breakdown, while a small value slows down the entire convergence process. Therefore, breakdowns, divergence and slow convergence are “detected” during the initial phase and the multiplier γ_0 is adapted accordingly:

Breakdowns : if the correction $\Delta U^{(k)}$ leads to a breakdown, then the iterate is not updated ($U^{(k+1)} = U^{(k)}$) while the exponential is modified by

$$\gamma^{(k+1)} = \frac{1}{2} \gamma^{(k)}, \quad \text{and} \quad \gamma_0 \leftarrow \frac{1}{2} \gamma_0.$$

Both the CFL and the multiplier are reduced. This procedure is repeated in case of successive breakdowns. When this happens, $\gamma^{(k)}$ and γ_0 tend to 0.

It should be noted that the Jacobian matrix remains unchanged at iteration $k + 1$. Hence, the computational cost of this iteration requires only the update of the preconditioner and the solution of a new linear system.

Divergence : A breakdown is seldom an isolated event and is usually preceded by instabilities during several iterations. Therefore, if any sign of convergence problem is encountered, it is safer to decrease the CFL number in advance to avoid unnecessary computations. We first define the relative correction $c^{(k)} = \Delta U^{(k)} / U^{(k)}$, where the division is taken component-wise and division by zero is discarded. The expert-system assumes that divergence occurs if the relative correction $c^{(k)}$ is large, a jump in the residual norm occurs, or if the linear system seems to be solved inaccurately. Hence, if any of the three following tests,

$$\begin{aligned} \|c^{(k)}\|_\infty &\geq 50\%, \\ \log\left(\frac{\|R^{(k+1)}\|_2}{\|R^{(k)}\|_2}\right) &> 0.5, \\ \|M^{(k)} \Delta U^{(k)} + R^{(k)}\|_2 &> \tau \|R^{(k)}\|_2, \end{aligned}$$

is verified, then, the CFL number is decreased

$$\gamma^{(k+1)} = 0.8 \gamma^{(k)},$$

but the multiplier is not modified. The parameter τ is a threshold used in the linear solver.

Slow convergence : Choosing a small γ_0 (or even $\gamma_0 = 0$) avoids the apparition of breakdowns but increases the length of the initial phase. Hence, to avoid a long initial phase, the multiplier is artificially increased at regular intervals.

Let s be a typical interval length and k_l the iteration index when the CFL strategy was last modified (due to a breakdown, ...). If for s iterations, the strategy remained unchanged (we are at iteration $k = k_l + s$), the multiplier increases while the interval length is shortened

$$\gamma_0 \leftarrow 2\gamma_0 \quad s \leftarrow \delta s,$$

where $\delta < 1$ is a reduction factor. Of course, the value of k_l is reset to k . We have set $s = 15$ and $\delta = 0.8$. The value of these parameters has little influence on the total length of the initial phase.

These three heuristic strategies completely define the behavior of $\gamma^{(k)}$ during the initial phase. Although breakdowns are avoided, it should be noted however that convergence can not be theoretically guaranteed. The initial iterate $U^{(0)}$ may be unrealistic or successive breakdowns may reduce $\gamma^{(k)}$ around 0 which gives an unreasonable number of iterations. In all our test cases though, convergence always occurred in a reasonable time.

The typical evolution of $\gamma^{(k)}$ using the three techniques described above is shown in Fig. 1b where a breakdown occurs at iteration k_1 , another is detected at k_2 , and γ_0 is increased at k_3 . The value of γ_0 can be evaluated from the slopes. The terminal phase begins at k_{switch} .

3.2 The terminal phase: k_{switch}

Under certain regularity conditions on $R(\cdot)$ and for an iterate close to the solution, Newton's method can be applied to (3), providing a quadratic convergence. When this happens, it suffices to use (4) by setting $\gamma^{(k)} = \infty$ (or $\gamma_1 = \infty$) [8]. Of course, the regularity of $R(\cdot)$ is a strong assumption and quadratic convergence is only an asymptotic result. In practical experiments, it is safer to select a bounded value of γ_1 allowing a smooth transition from the initial to the terminal phases. We have chosen

$$\gamma_1 = 2\gamma_0,$$

which is subsequently doubled every two iterations.

The main problem is to verify if an iterate is close to the solution. There is no definite answer and we must rely again on some heuristics. With SER, we have observed that monitoring $\|R(U)\|_2$ alone is not sufficient since it may lead to oscillations. In the expert-system, several metrics are combined into a single value that estimates the "quality" of $U^{(k)}$:

- The first metric is the relative norm of the residual

$$m_1^{(k)} = -\log \left(\frac{\|R^{(0)}\|_2}{\|R^{(k)}\|_2} \right).$$

It usually ranges between 0 and 16 (the latter corresponds to the machine precision).

- Again $c^{(k)} = \Delta U^{(k)}/U^{(k)}$ represents the relative correction. The second metric measures the amount of correction by

$$m_2^{(k)} = -\log \left(\|c^{(k)}\|_2 \right).$$

When $m_2^{(k)} \simeq 1$, the correction is about one order of magnitude smaller than the iterate vector. At convergence, $m_2^{(k)}$ is close to 4.

- The third metric is the speed at which $m_2^{(k)}$ increases

$$m_3^{(k)} = \text{slope} \left(m_2^{(k)} \right).$$

The function $\text{slope}(\cdot)$ returns the slope obtained by linear regression over the last few values. At the beginning of the iterations, convergence has not begun and $m_3^{(k)}$ is close to 0. In the terminal phase, a value of 2 denotes quadratic convergence.

- The last metric comes from geometrical considerations. If the fluid has a constant state at the beginning of the simulation, then a perturbation is first located along some boundaries and propagates slowly to the entire domain. From a numerical point of view, it means that $\Delta U^{(k)}$ has only a few non-zero components at the beginning and this proportion grows to a maximum (note that this maximum may not be 100% as this happens for supersonic computations where the nodes near the supersonic inlet remain unchanged). Therefore, we define

$$m_4^{(k)} = 1 - \text{slope} \left(\text{nnz}(\Delta U^{(k)}) \right).$$

The function $\text{nnz}(\cdot)$ returns the number of non-zero components of a vector. This metric tends to 1 when the flow features have been correctly computed.

These four metrics taken separately give an idea of the convergence. To obtain more reliability, they are combined in a weighted sum

$$m^{(k)} = \sum_{i=1}^4 \alpha_i m_i^{(k)},$$

and a moving average over the last $K = 10$ iterations is taken

$$\overline{m}^{(k)} = \frac{1}{K} \sum_{j=0}^{K-1} m^{(k-j)}, \quad (6)$$

to reduce the local variations. The weights are chosen to give a similar influence to every term (we have selected empirically $\alpha = [1, 2, 8, 16]$).

The typical evolution of $\overline{m}^{(k)}$ is given in Fig. 1a. In the initial phase, no convergence happens and all metrics remain almost constant. Then, convergence begins gradually and $\overline{m}^{(k)}$ increases. When it reaches a certain threshold ($\overline{m}^{(k)} > 15\overline{m}^{(K)}$), the iterate is considered sufficiently close and the expert-system switches to the terminal phase.

4 Residual Distribution Method

The expert-system presented in the previous section has been implemented into numerical codes based on the residual distribution method. The residual distribution method was originally proposed by Roe [10] and further developed by Roe, Deconinck and their co-workers. We present a brief overview of the principles of the method. Further details can be found in [11, 12, 13] and the references therein.

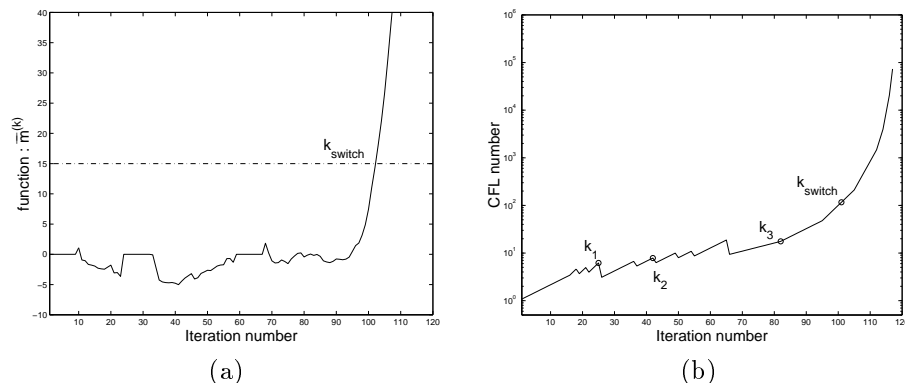


Figure 1: Metrics of the expert-system: (a) Evolution of $\overline{m}^{(k)}$ for the determination of k_{switch} and, (b) typical evolution of $\gamma^{(k)}$.

For the sake of simplicity, we describe the 2D case but the 3D generalization is straightforward. Given a triangulation of the computational domain, the solution of (1) is approximated by piecewise linear functions,

$$U(x, y, t) = \sum_i U_i(t) N_i(x, y), \quad (7)$$

where $U_i(t)$ is the time dependent nodal value of the state variables at node i and $N_i(\cdot)$ is the corresponding piecewise linear shape function with compact support. In quasi-linear form, (1) reads

$$\frac{\partial U}{\partial t} + A_U \frac{\partial U}{\partial x} + B_U \frac{\partial U}{\partial y} = S,$$

where A_U and B_U are the convective flux Jacobian matrices. Integration of the above expression over a triangle T defines the total fluctuation (also called *cell residual*) as

$$\Phi^T = - \iint_T \frac{\partial U}{\partial t} dV = \Phi_C^T - \Phi_S^T, \quad (8)$$

where the convective residual Φ_C^T and the source term residual Φ_S^T are given by

$$\Phi_C^T = \iint_T \left(A_U \frac{\partial U}{\partial x} + B_U \frac{\partial U}{\partial y} \right) dV, \quad \text{and} \quad \Phi_S^T = \iint_T S dV.$$

In the residual distribution approach, the total fluctuation is distributed to the three nodes defining the cell. More precisely, every node i of cell T receives a fraction of the convective residual Φ_C^T ,

$$\Phi_C^{T,i} = \beta_C^{T,i} \Phi_C^T, \quad (9)$$

where the convective distribution matrices satisfy

$$\sum_{i \in T} \beta_C^{T,i} = \hat{I}$$

for consistency reasons. A similar treatment is applied to the source term residual. The choice of the distribution matrices is central in the residual approach and this treatment is deferred until Section 4.2. Finally, summing (8) over all cells T adjacent to node i , using (7) and (9), and integrating leads to the semi discrete form

$$\frac{dU_i}{dt} = -\frac{1}{S_i} \sum_{T \in i} \left(\beta_C^{T,i} \Phi_C^T - \beta_S^{T,i} \Phi_S^T \right)$$

for node i where S_i represents the area of the median dual cell around node i . This latter expression is equivalent to (2).

4.1 Evaluation of convective residuals

Since the components of the state vector U have linear variation in cell T , following the procedure of a conservative linearization [12, 14], the convective cell residual can be written as

$$\Phi_C^T = \sum_{i \in T} K_i U_i,$$

where the summation is performed over the three nodes defining the cell T . The vector U_i is the solution at node i and the matrix K_i is a linear combination of the flux Jacobian matrices taken in an averaged state of U

$$K_i = \frac{1}{2} (A_U n_{x,i} + B_U n_{y,i}),$$

where $n_{x,i}$ and $n_{y,i}$ are the components of the normal vector of the boundary edge of cell T opposite to node i scaled by the length of the edge (see Fig. 2). If the left-hand-side of (1) is hyperbolic, then the matrix K_i has real eigenvalues and a complete set of left and right real eigenvectors. Its diagonalization yields

$$K_i = \frac{1}{2} R_i \Lambda_i L_i,$$

where the columns of R_i (rows of L_i resp.) contain the right (left resp.) eigenvectors of K_i and Λ_i is the diagonal matrix of the eigenvalues. The eigenvalue matrix can be written as $\Lambda_i = \Lambda_i^+ + \Lambda_i^-$, with $\Lambda_i^\pm = (\Lambda_i \pm |\Lambda_i|)/2$. The generalized upwind parameters $K_i^+ = R_i \Lambda_i^+ L_i$ and $K_i^- = R_i \Lambda_i^- L_i$ play an important role in the multidimensional upwinding of the residual distribution schemes, as we will show below.

4.2 Distribution of the Convective Residual

The definition of the convective distribution matrices $\beta_C^{T,i}$ plays a crucial role and is the topic of an on-going research. Various schemes exist focussing on multidimensional upwinding, linearity, positivity and other special properties. The

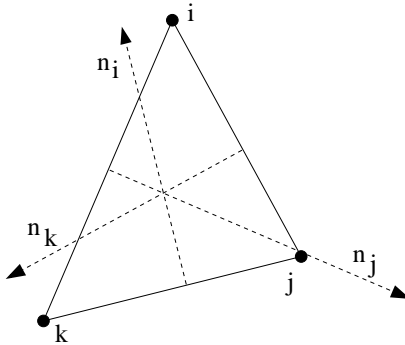


Figure 2: Definition of a cell with three nodes i , j , and k and the associated scaled normals.

narrow scheme (N-scheme in short) used in this paper is a multidimensional upwind scheme. In the scalar case, it means that the residual is distributed entirely to the downstream nodes [15]. Physically, this is motivated by the fact that the waves propagate away from upstream nodes and those should therefore not be influenced. Mathematically, the distribution function for the N-scheme can be expressed by

$$\Phi_C^{T,i} = \beta_C^{T,i} \Phi_C^T = K_i^+(U_i - U_{in}),$$

where $U_{in} = (\sum K_i^-)^{-1} \sum K_i^- U_i$ is the interpolated inflow state. The N-scheme is linear and positive and produces the smallest cross-diffusion in its class. Consequently, it captures shocks in a monotonic manner, but its accuracy remains first order only.

4.3 Distribution of the Source Term Residual

For the Navier-Stokes equations, computation and distribution of the source term residual Φ_S require a different approach than the one described in the previous paragraph. It is based on a Petrov-Galerkin interpretation of residual distribution schemes. For the description of the method, including the treatment of boundary conditions, the reader is directed to the work of van der Weide [15].

The ideal magnetohydrodynamics equations are solved in a non-conservative invariant form containing Powell's source term. This way the singularities present in the Jacobian matrices A_U and B_U are removed, which is essential in the framework of residual distribution methods. A detailed description of the technique is given in [14, 16].

5 Numerical experiments

The expert-system has been tested on a wide variety of test cases using the Euler, Navier-Stokes and MHD equations. Four unstructured geometries are considered,

both in 2 and 3 dimensions. The numerical experiments use two simulation softwares based on the residual distribution (fluctuation splitting) spatial discretization technique. Euler and Navier-Stokes computations are obtained with the THOR code developed at the von Karman Institute [13, 17], while ideal MHD computations use the RA code written by the second author.

5.1 Test cases

We have selected 7 representative test cases using three sets of equations and four geometries.

Euler : The Euler equations describe the behavior of an inviscid fluid. They derive from the physical principles of mass conservation, Newton's second law and energy conservation. In conservative form they are written as

$$\frac{\partial}{\partial t} \begin{pmatrix} \rho \\ \rho \mathbf{v} \\ E \end{pmatrix} + \nabla \cdot \begin{bmatrix} \rho \mathbf{v} \\ \rho \mathbf{v} \mathbf{v} + \hat{I} p \\ (E + p) \mathbf{v} \end{bmatrix} = 0, \quad (10)$$

where \hat{I} is the unit matrix, ρ is the density, \mathbf{v} is the velocity vector, p is the thermal pressure and E is the total energy density defined by

$$E = \frac{p}{\gamma - 1} + \frac{1}{2} \rho \mathbf{v} \cdot \mathbf{v}.$$

The constant γ denotes the ratio of specific heats.

Navier-Stokes : The set of Navier-Stokes equations applies to viscous flows, including dissipation, transport phenomena of viscosity and thermal conduction. It differs from the Euler equations by its non vanishing right-hand-side

$$S = \nabla \cdot \mathbf{F}^\nu,$$

where \mathbf{F}^ν is the viscous flux vector. This vector is a function of the viscous stress tensor τ and the heat flux vector \mathbf{q} .

Ideal Magnetohydrodynamics : The ideal MHD equations govern the motion of conducting fluids under the presence of a magnetic field in case of infinite conductivity. They couple the Euler equations of hydrodynamics to Maxwell's equations of electrodynamics. In conservative form the hyperbolic set of ideal MHD equations is given by

$$\frac{\partial}{\partial t} \begin{pmatrix} \rho \\ \rho \mathbf{v} \\ \mathbf{B} \\ E \end{pmatrix} + \nabla \cdot \begin{bmatrix} \rho \mathbf{v} \\ \rho \mathbf{v} \mathbf{v} + \hat{I}(p + \mathbf{B} \cdot \mathbf{B}/2) - \mathbf{B} \mathbf{B} \\ \mathbf{v} \mathbf{B} - \mathbf{B} \mathbf{v} \\ (E + p + \mathbf{B} \cdot \mathbf{B}/2) \mathbf{v} - \mathbf{B}(\mathbf{v} \cdot \mathbf{B}) \end{bmatrix} = 0, \quad (11)$$

where \mathbf{B} is the magnetic vector field and E is the total energy density defined as

$$E = \frac{p}{\gamma - 1} + \frac{1}{2} \rho \mathbf{v} \cdot \mathbf{v} + \frac{1}{2} \mathbf{B} \cdot \mathbf{B}.$$

Equation (11) describes the conservation of mass, momentum, magnetic flux and energy. It has to be supplemented by the solenoidal condition of the magnetic field, stating that magnetic monopoles do not exist

$$\nabla \cdot \mathbf{B} = 0.$$

The quasi-linear form of (11) contains singular Jacobian matrices and it is therefore not invariant to Gallilean transformations. In 1972, Godunov proved, that the only symmetrizable form of the ideal MHD equations contains the following source term [18]

$$S = - \begin{pmatrix} 0 \\ \mathbf{B} \\ \mathbf{v} \\ \mathbf{v} \cdot \mathbf{B} \end{pmatrix} \nabla \cdot \mathbf{B},$$

which is proportional to the divergence of the magnetic field. This alternative form is the Gallilean invariant form of the ideal MHD equations. It was also shown by Powell that this form is numerically more stable [19].

The set of equations above is solved on the following geometries:

Nozzle flow : We consider the simple test case of a hypersonic flow through a converging diverging nozzle (Fig. 5.1a). For the MHD equations this test case was first proposed by Vanden Abeele [20]. Uniform flow enters the nozzle from the left and leaves it at the right. The flow is fully supersonic and superfast in the nozzle, corresponding to the Euler and ideal MHD equations, respectively. Because of symmetry, we simulate the flow in the upper part only. At the top of the nozzle we impose inviscid wall boundary conditions for the Euler equations and perfectly conducting inviscid wall boundary conditions for the ideal MHD equations. Initially, the following uniform flow fields are prescribed: density $\rho = 1$, momentum vector $\rho\mathbf{v} = (1, 0, 0)$, total energy density $E = 0.9$ for the Euler equations and density $\rho = 1.5$, momentum vector $\rho\mathbf{v} = (4, 0, 0)$, magnetic field vector $\mathbf{B} = (2, 0, 0)$ and total energy density $E = 14.9$ for the ideal MHD equations. The grid contains 5712 cells and 3015 nodes.

Bow shock flow : 2D bow shock flow simulations serve as basic building blocks of hypersonic blunt body simulations in hydrodynamics and of space physics applications in MHD. The latter application includes bow shock simulations over planets, comets or coronal mass ejections. Because of symmetry, we only simulate the flow field over the upper left quadrant of a cylinder, and the solution is symmetric with respect to the horizontal axis (Fig. 5.1b). Initially we impose the following uniform flow fields: density $\rho = 1$, momentum vector $\rho\mathbf{v} = (1, 0, 0)$, total energy density $E = 0.7$ for the Euler equations and density $\rho = 1$, momentum vector $\rho\mathbf{v} = (6, 0, 0)$, magnetic field vector $\mathbf{B} = (0.5, 0, 0)$, total energy density $E = 19.625$ for the ideal MHD equations. The grid contains 6152 cells and 3203 nodes.

NACA airfoil : We compute the well documented 2D hydrodynamic test case of a subsonic flow over a NACA-0012 airfoil [21, 11, 15] (Fig. 5.1c). Initially we impose Mach number $M_\infty = 0.83$, angle of attack $\alpha = 2^\circ$ and free stream temperature $T_\infty = 273.15 K$. We perform inviscid and laminar viscous flow computations. In the latter case the Reynolds number is $Re = 5000m^{-1}$. The grid contains 10924 cells and 5590 nodes.

Ogive Cylinder : The flow field around an ogive cylinder was experimentally investigated by ONERA for several angles of incidence [22] (Fig. 5.1d). This 3D test case was numerically computed by van der Weide [15, 12] for the angle of incidence $\alpha = 10^\circ$. The initial conditions of this test case are the following: Mach number $M_\infty = 2$, angle of incidence $\alpha = 10^\circ$, free stream temperature $T_\infty = 183 K$ and Reynolds number $Re_\infty = 5.33 \cdot 10^6 m^{-1}$. The grid contains 1 039 022 cells and 177 846 nodes.

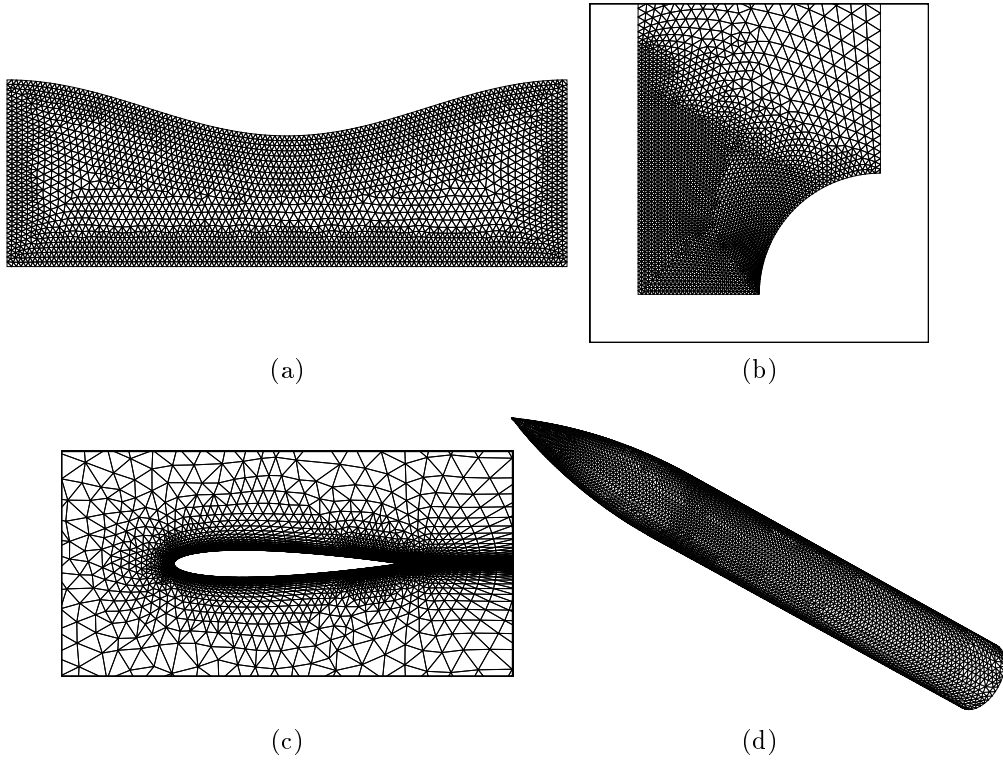


Figure 3: Grids used for the validation of the Expert-System: (a) Nozzle, (b) Bow shock detail, (c) NACA airfoil detail, and (d) 3D Ogive cylinder — trace of the grid on the body.

5.2 Experiments

The ultimate goal of the expert-system is to provide a net gain in terms of computation time. However, timings results are always hazardous to present since every simulation depends on many factors. For these test cases for example, the computation time depends on the number of Jacobian evaluations, the number of times the preconditioner has to be constructed and the total number of linear iterations. All these values depend in turn on the particular choice of the preconditioner, the parameters of the inexact Newton's method, etc. In these experiments, the Jacobian matrices are evaluated numerically while the linear systems are solved iteratively with a threshold $\tau = 10^{-5}$ using a block incomplete LU factorization.

In the following, the three strategies are compared in terms of total number of linear systems to be solved. This corresponds to the number of non-linear iterations or Jacobian evaluations for SER and EXP. For the expert-system, the number of Jacobian evaluations is overestimated since some matrices are reused in case of a breakdown.

Unless otherwise stated, the values of γ_{SER} and γ_{EXP} are determined — by trial and error — to give the lowest number of iterations. Thanks to the robustness of the expert-system, the initial value γ_0 has little influence. It was set arbitrarily to $\gamma_0 = 1$. Of course, a user-tuned parameter provides a better convergence. The maximum value of the CFL is set to $\gamma_{max} = 10^6$.

5.3 Typical result

Figure 4 presents the typical evolution of the CFL number and the convergence history for the solution of the Euler equations around a NACA airfoil. Convergence is obtained in 67 iterations with EXP, 47 iterations with SER and goes down to 34 with the expert-system.

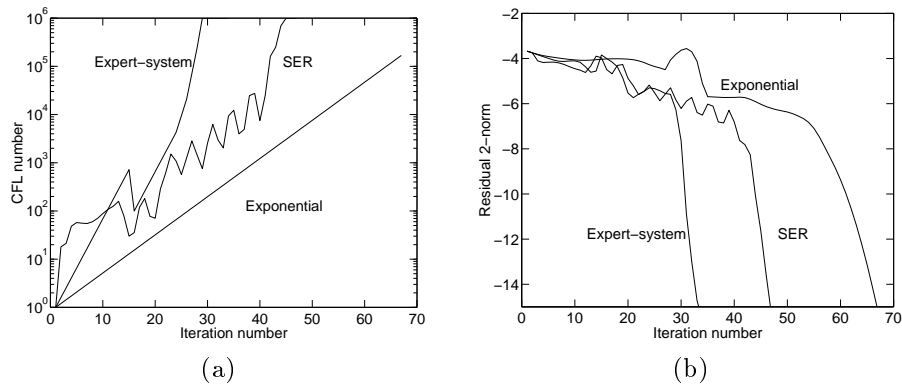


Figure 4: Convergence history of the transient solution of the Euler equations around a NACA airfoil for the three CFL strategies: (a) CFL history, and (b) residual norm history.

Obviously, the exponential law is not optimal. Indeed, we have to choose a rather small γ_{EXP} to avoid breakdowns in the initial phase. Hence, $\gamma^{(k)}$ is still small when $U^{(k)}$ is close to the solution, resulting in a slow convergence rate in the terminal phase. Selecting a larger γ_{EXP} is not possible since it produces a breakdown in the initial phase around $k = 25$.

For this problem, the SER strategy converges faster than EXP but the presence of oscillations results in extra iterations. On the other hand, close to the solution, large CFL numbers are chosen and a fast convergence is observed.

By detecting that $U^{(k)}$ is close to the solution, the expert-system produces large CFL numbers early, leading to fast convergence. Convergence happens after 34 iterations, which is 25% faster than SER and two times faster than EXP. In the history of the CFL number, we observe that a divergence is detected for $k = 16$. This corresponds to a slight jump in the residual norm.

All three strategies have a similar convergence history in the initial phase when flow features are not well resolved. Hence, if a mild convergence criterion is set (around $\|R^{(k)}\|_2 \leq 10^{-6}$), the gain of the expert-system is less impressive.

5.4 Robustness

A proper choice of the initial parameters is crucial to limit the total number of non-linear iterations. For the SER or exponential strategies, the values of γ_{SER} and γ_{EXP} must also be small enough to avoid breakdowns.

Figure 5 shows the total number of iterations as a function of the initial parameter for the Euler flow around a NACA airfoil. The ‘o’ symbol means that a converged solution was obtained while the ‘x’ symbol denotes a breakdown.

For both SER and EXP, the parameter space for the initial parameter can be divided in two zones separated by a threshold. Below the threshold, the iteration converges while breakdowns occur above the threshold (due to finite precision arithmetic, there is a small zone around the threshold where convergence and breakdown alternate). In the first zone, the function has a large negative slope which denotes an annoying sensitivity to the value of the initial parameter. If a good estimate of the initial parameter is not available, the number of iterations can be severely sub-optimal.

On the other hand, the expert-system proves to be very robust. Not only convergence was always observed for all our test cases, but also, the number of iterations is less sensitive to the value of γ_0 (Fig. 5a).

5.5 Validation

Since the expert-system is heuristic in nature, it can only be validated empirically by comparison with other strategies on many problems. Table 1 presents iteration counts obtained on the seven test cases for the three strategies. For SER and EXP, iteration counts are given using the “optimal” value of the parameter and for a value of the parameter roughly 10% below the optimum. For the expert system, the fixed value $\gamma_0 = 2$ is used. Also, to give an idea on the sub-optimality, the

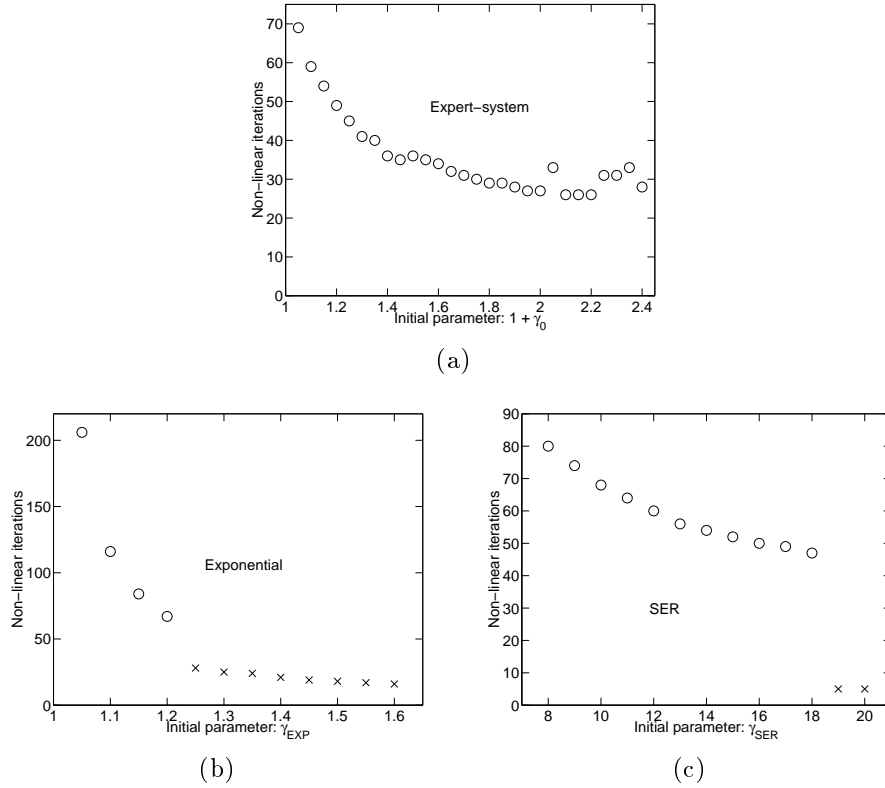


Figure 5: Robustness of the CFL strategies measured by the number of total non-linear of iterations as a function of the initial parameter: (a) Expert-system, (b) Exponential law, and (c) SER strategy.

best value is also given in parenthesis. The best value over all three strategies is denoted in **bold** letters.

On average, the expert-system provides a reduction in the total number of iterations. The reduction is larger for complex problems requiring many iterations. Indeed, for the bow shock, the initial phase takes about 100 iterations to locate correctly the shock. During this initial phase, the values of $\gamma^{(k)}$ must remain small, which forces the initial parameters to be small and reduces the convergence rate of SER and EXP. On the other hand, the expert-system correctly detects when a good iterate is obtained ($k_{switch} \simeq 100$) and produces larger subsequent values of $\gamma^{(k)}$.

For the nozzle problem, the expert-system fails to provide any improvements at all. On the contrary, it requires 25% more iterations. This is caused by three factors: the problem is relatively easy in the sense that few iterations are needed for convergence. Still, the moving average (6) requires K iterations before estimating the quality of the iterate. Next, large value of γ_{EXP} and γ_{SER} can be taken. In this

Geometry	Equation	SER		Exponential		Expert-system	
		γ_{SER}	#iter	γ_{EXP}	#iter	$1 + \gamma_0$	#iter
Nozzle	Euler	36	17	3.8	16	2.0	23
		35	17	3.7	16	(3.8	18)
	MHD	14	17	4.3	14	2.0	18
		15	17	4.2	14	(4.1	14)
Naca	Euler	18	47	1.20	67	2.0	27
		17	49	1.15	84	(2.2	26)
	N-S	40	32	1.6	28	2.0	30
		36	38	1.4	33	(2.2	29)
Bow	Euler	2.4	139	1.04	185	2.0	111
		2.3	143	1.03	255	(1.7	92)
	MHD	3.2	142	1.04	157	2.0	129
		3.1	158	1.03	189	(1.09	117)
Ogive	N-S	5.0	26	1.6	24	2.0	23
		4.5	32	1.5	27	(2.4	19)

Table 1: Comparison of the three strategies for 7 test-cases with different values of the initial parameters.

experiment, we have set $\gamma_0 = 2$ and this limits the growth of $\gamma^{(k)}$. Finally, a shock suddenly builds up at iteration 4. It is erroneously considered as a divergence by the expert-system that reduces the CFL in the next iteration.

For moderately difficult problems, the expert-system provides convergence similar to the other strategies. Of course, tuning the initial parameter gives better performance.

6 Discussion and conclusion

We have presented a new strategy for the automatic adaptation of the CFL number during the iterative solution of hyperbolic PDE's by implicit upwind methods. This strategy contains many heuristics — hence the name *expert-system* — that attempt to avoid breakdowns of the iteration while providing an acceptable convergence rate. Compared to existing strategies such as the exponential law or the Switch Evolution Relaxation, the expert-system proves to be more efficient: (a) robustness is increased in the sense that the number of non-linear iterations is not much affected by the choice of parameters, and (b) convergence is usually faster with the system than with other strategies.

Based on our experience, the gain obtained by using the expert-system is larger when the problem is more complex, requiring many iterations or when the tolerance criterion on the residual vector is small. On the other side, when a maximum value of the CFL numbers is needed for stability reasons, or when convergence can not be obtained to a good accuracy, the benefits of the expert-system will remain limited.

Acknowledgements

The authors are grateful to Kurt Sermeus, Herman Deconinck (von Karman Institute), and Stefaan Poedts (Center for Plasma-Astrophysics, K.U.Leuven) for their valuable inputs and for providing access to the THOR code for the numerical solution of the Euler and Navier-Stokes equations.

This work is funded by the *Fonds voor Wetenschappelijk Onderzoek* (FWO project G0344.98: “Multidimensional upwinding and parallel implicit solvers for MHD”) and by the UIAP P4/02 Interuniversity Poles of Attraction, initiated by the Belgian State, Prime Minister’s Office for Science Technology and Culture. The scientific responsibility rests with its authors.

References

- [1] J. E. Dennis and R. B. Schnabel Jr. *Numerical Methods for Unconstrained Optimization and Nonlinear Equations*. Prentice-Hall Inc., Englewood Cliffs, New-Jersey, 1983.
- [2] C. T. Kelley. *Iterative Methods for Linear and Nonlinear Equations*. Frontiers in Applied Mathematics, SIAM, 1995.
- [3] C. T. Kelley and D. E. Keyes. Convergence analysis of pseudo-transient continuation. *SIAM J. Num. Anal.*, Vol. 35, No. 2, pp. 508–523, 1998.
- [4] E. Issman and G. Degrez. Implicit iterative methods for a multidimensional upwind Euler/Navier-Stokes solver on unstructured meshes. Technical Report 1995-14, von Karman Institute (Belgium), 1995.
- [5] W. Mulder and B. van Leer. Experiments with implicit upwind methods for the Euler equations. *J. Comput. Phys.*, Vol. 59, pp. 232–402, 1985.
- [6] J. A. Essers, M. Delanaye, and P. Rogiest. An upwind biased finite volume technique for solving compressible Navier-Stokes equations on irregular meshes. *AIAA Journal*, Vol. 33, No. 5, pp. 833–842, 1995.
- [7] Z. Johan, T. J. R. Hughes, and F. Shakip. A globally convergent matrix-free algorithm for implicit time-marching schemes arising in finite element analysis in fluids. *Comp. Meth. in Appl. Mech. and Eng.*, Vol. 87, pp. 281–304, 1991.
- [8] A. Ern, V. Giovangigli and D. E. Keyes, and M. D. Smooke. Towards polyalgebraic linear system solvers for nonlinear elliptic problems. *SIAM J. Sci. Comput.*, Vol. 15, pp. 681–703, 1994.
- [9] E. Issman, G. Degrez, and H. Deconinck. Implicit upwind residual distribution Euler/Navier-Stokes solver on unstructured grids. *AIAA Journal*, Vol. 34, No. 10, pp. 2021, 1996.
- [10] P. L. Roe. Fluctuations and signals – a framework for numerical evolution problems. In *Numerical Methods for Fluid Dynamics*. Academic Press, 1982.

- [11] H. Paillère, H. Deconinck, and P. L. Roe. Conservative upwind residual distribution schemes based on the steady characteristics of the Euler equations. *AIAA*, Vol. CP-951700, pp. 592, 1995.
- [12] E. van der Weide, E. Issman, H. Deconinck, and G. Degrez. Parallel, implicit, multi-dimensional upwind, residual distribution method for the Navier-Stokes equations on unstructured grids. *Computational Mechanics*, Vol. 23, No. 2, pp. 199–208, 1999.
- [13] E. van der Weide and H. Deconinck. Positive matrix distribution schemes for hyperbolic systems, with application to the Euler equations. In *Proceedings of the 3rd European CFD Conference*, pp. 747–753. Wiley, 1996.
- [14] Á. Csík, H. Deconinck, and S. Poedts. Monotone residual distribution schemes for the ideal 2D magnetohydrodynamic equations on unstructured grids. In *14th AIAA Conference*, pp. 99–3325, 1999.
- [15] E. van der Weide. *Compressible Flow Simulation on Unstructured Grids using Multi-dimensional Upwind Schemes*. PhD thesis, Technical University Delft, The Netherlands, 1998.
- [16] Á. Csík, H. Deconinck, and S. Poedts. On the shock capturing properties of the non-conservative symmetrizable form of the ideal magnetohydrodynamic equations. *Journal of Computational Physics*, 2000 (submitted).
- [17] E. van der Weide and H. Deconinck. Upwind Residual Distribution Methods for Compressible Flow: An Alternative to Finite Volume and Finite Element Methods; Part II: System Schemes and Applications. In *VKI LS 1997-02, Computational Fluid Dynamics*, 1997.
- [18] S. K. Godunov. Nonlinear hyperbolic problems. In C. Carasso, P. A. Raviart, and D. Serre, editors, (*advanced research workshop*) *Lecture Notes in Mathematics*, volume 1270. Springer-Verlag, 1987.
- [19] K. G. Powell, P. L. Roe, R. S. Myong, T. I. Gombosi, and D. L. De Zeeuw. An upwind scheme for magnetohydrodynamics. *AIAA Paper*, pp. 95–1704–CP, 1995.
- [20] D. Vanden Abeele and H. Deconinck. Development of a Godunov-type solver for ideal two-dimensional MHD. Technical Report 1995-13, von Karman Institute, 1995.
- [21] H. Viviand. Numerical solutions of two-dimensional reference test cases. AGARD Advisory Report No. 211, 1985.
- [22] AGARD Advisory Report no 303. a selection of experimental test cases for the validation of CFD codes. AGARD, 1994.